



The Epstein-Barr Virus Oncogene EBNA1 Suppresses Natural Killer Cell Responses and Apoptosis Early after Infection of Peripheral B Cells

Danielle Westhoff Smith,^a Adityarup Chakravorty,^b Mitch Hayes,^b  Wolfgang Hammerschmidt,^c  Bill Sugden^b

^aDepartment of Surgery, Medical School, University of Minnesota, Minneapolis, Minnesota, USA

^bMcArdle Laboratory for Cancer Research, University of Wisconsin–Madison, Madison, Wisconsin, USA

^cResearch Unit Gene Vectors, Helmholtz Zentrum München, German Research Center for Environmental Health and German Center for Infection Research (DZIF), Munich, Germany

Danielle Westhoff Smith and Adityarup Chakravorty contributed equally to this work. Author order was chosen in reverse alphabetical order.

ABSTRACT The innate immune system serves as frontline defense against pathogens, such as bacteria and viruses. Natural killer (NK) cells are a part of innate immunity and can both secrete cytokines and directly target cells for lysis. NK cells express several cell surface receptors, including NKG2D, which bind multiple ligands. People with deficiencies in NK cells are often susceptible to uncontrolled infection by herpesviruses, such as Epstein-Barr virus (EBV). Infection with EBV stimulates both innate and adaptive immunity, yet the virus establishes lifelong latent infection in memory B cells. We show that the EBV oncogene EBNA1, previously known to be necessary for maintaining EBV genomes in latently infected cells, also plays an important role in suppressing NK cell responses and cell death in newly infected cells. EBNA1 does so by downregulating the NKG2D ligands ULBP1 and ULBP5 and modulating expression of c-Myc. B cells infected with a derivative of EBV that lacks EBNA1 are more susceptible to NK cell-mediated killing and show increased levels of apoptosis. Thus, EBNA1 performs a previously unappreciated role in reducing immune response and programmed cell death after EBV infection, helping infected cells avoid immune surveillance and apoptosis and thus persist for the lifetime of the host.

IMPORTANCE Epstein-Barr virus (EBV) is a ubiquitous human pathogen, infecting up to 95% of the world's adult population. Initial infection with EBV can cause infectious mononucleosis. EBV is also linked to several human malignancies, including lymphomas and carcinomas. Although infection by EBV alerts the immune system and causes an immune response, the virus persists for life in memory B cells. We show that the EBV protein EBNA1 can downregulate several components of the innate immune system linked to natural killer (NK) cells. This downregulation of NK cell activity translates to lower killing of EBV-infected cells and is likely one way that EBV escapes immune surveillance after infection. Additionally, we show that EBNA1 reduces apoptosis in newly infected B cells, allowing more of these cells to survive. Taken together, our findings uncover new functions of EBNA1 and provide insights into viral strategies to survive the initial immune response postinfection.

KEYWORDS B cell, Epstein-Barr virus, ULBP, c-Myc, herpesviruses, innate immunity, natural killer cells

The innate immune system can be activated by both external invaders, including fungi, bacteria, and viruses, and internal stimuli, such as cellular stress or malignancies (1, 2). This system is complex, with one component, natural killer (NK) cells, being able both to secrete immune-activating cytokines, such as gamma interferon and

Citation Westhoff Smith D, Chakravorty A, Hayes M, Hammerschmidt W, Sugden B. 2021. The Epstein-Barr virus oncogene EBNA1 suppresses natural killer cell responses and apoptosis early after infection of peripheral B cells. *mBio* 12:e02243-21. <https://doi.org/10.1128/mBio.02243-21>.

Invited Editor Erle S. Robertson, Perelman School of Medicine at the University of Pennsylvania

Editor Stacey Schultz-Cherry, St. Jude Children's Research Hospital

Copyright © 2021 Westhoff Smith et al. This is an open-access article distributed under the terms of the [Creative Commons Attribution 4.0 International license](https://creativecommons.org/licenses/by/4.0/).

Address correspondence to Bill Sugden, sugden@oncology.wisc.edu.

Received 2 August 2021

Accepted 14 October 2021

Published 16 November 2021

tumor necrosis factor alpha, and to recognize and kill target cells directly (3). NK cells constitute between 5 and 20% of circulating lymphocytes in humans (4) and express several receptors on their surface, including the NKG2D receptor, which can bind to a number of cognate major histocompatibility complex class I (MHC-I)-like ligands (5). NKG2D is an activating molecule, and its binding to ligands can lead to direct killing of the cells expressing those ligands (6). Typically, cells express relatively low levels of NKG2D ligands, but their expression can be upregulated by stress, transformation, or pathogens (7, 8). Members of one family of viruses, the herpesviruses, have been found to regulate individual ligands of the NKG2D family transcriptionally and posttranscriptionally, and patients with NK cell deficiencies often have uncontrolled herpesvirus infections (9–11), highlighting the importance of NK cells in limiting herpesvirus illnesses.

Epstein-Barr virus (EBV) is an oncogenic herpesvirus that infects 90 to 95% of the world's adult population and causes a variety of B-cell and epithelial cell malignancies in a subset of infected people (12). In tumor cells, EBV is mostly latent, and during latency a variable subset of viral genes is expressed, including minimally one set of viral microRNAs (miRNAs) (BARTs), two noncoding RNAs (the EBERs), and one viral protein, EBNA1 (13). Initial infection with EBV leads to various immune responses, including expansion of CD8⁺ T cells directed against viral antigens and activation of specific subtypes of NK cells (14, 15). Additionally, infection of B cells with EBV can activate the ATR/Chk1 (16–18) and/or the ATM/Chk2 (19) pathway, concomitant with a subset of the infected cells undergoing a period of rapid cell division (17, 19). Activation of these pathways is known to upregulate expression of ligands that can bind the NKG2D receptor and activate NK cells (7). However, in spite of activating various components of the immune system, at least some EBV-positive cells evade the host immune response and survive lifelong in humans.

While EBV has evolved pathways to regulate the host immune response, the majority of viral genes linked to immune evasion or suppression are typically expressed during the lytic or productive phase of the viral life cycle (20). Some lytic genes, such as *BCRF1* and *BNLF2a*, are also expressed early after infection and can inhibit both NK and T cell activity against newly EBV-positive cells (21, 22). However, only a few of EBV's well-studied latent gene products have been linked to immune evasion or suppression (23–25). The EBV latent protein EBNA1 binds sequence-specifically to both viral and cellular DNA (26–28). EBNA1 mediates maintenance of EBV's genomes in latently infected cells (29, 30) and can both enhance and inhibit transcription of viral and cellular genes (31–36). The EBNA1 protein contains a long glycine-alanine (Gly-Ala) repeat region that has been linked to inhibiting both its own translation and processing for antigen presentation (37–39). However, no *trans*-acting immune evasion functions have been attributed to EBNA1, which is expressed in all EBV-positive cells. We now show that EBNA1 directly inhibits the expression of both NKG2D ligands and c-Myc by binding cellular DNA near the transcription start sites of these genes. EBNA1's binding each of these genomic sites enhances the capacity of newly infected cells to evade host immune responses and to survive and proliferate. We have uncovered a vital addition to EBV's repertoire of immune evasion strategies that allows virus-positive cells to bypass immune responses and persist for the lifetime of the host.

RESULTS

EBNA1 directly regulates the expression of the NKG2D ligand ULBP1. When the NKG2D receptor on NK cells binds its ligands, it can activate cytotoxic T cells and/or directly kill the target cells (40, 41). We first screened available transcriptome sequencing (RNA-seq) data (42) to determine the expression patterns of NKG2D ligands in the first 8 days after B cells are infected with EBV *in vitro*. Only the NKG2D ligand ULBP1 was upregulated immediately after EBV infection and subsequently downregulated (Fig. 1A). While we also detected expression of the ligands MICA and MICB, their levels did not change appreciably within the first 8 days after EBV infection (Fig. 1A). We show that downregulation of ULBP1 after the initial increase in its expression after EBV

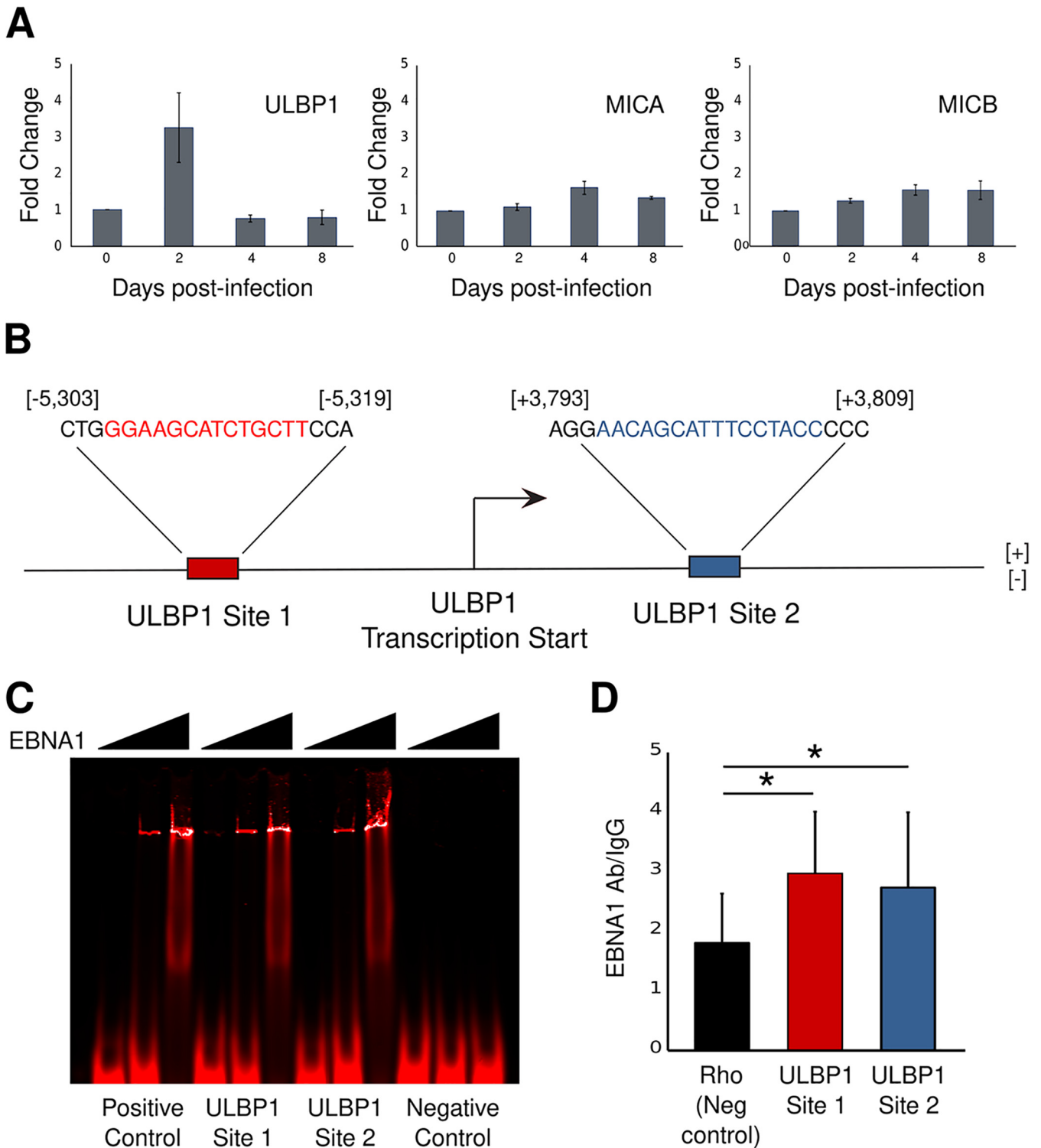


FIG 1 EBNA1 binds cellular DNA near the ULBP1 transcription start site. (A) Levels of ULBP1 increase soon after EBV infection of primary B cells and quickly decline to initial levels. Levels of MICA and MICB do not change significantly. ULBP2 to -6 mRNAs were below the detection threshold (below 25 normalized reads on average). Data are derived from <http://ebv-b.helmholtz-muenchen.de/>. (B) EBNA1 PWM-predicted binding sites (red and blue sequences) associated with the NKG2D ligand ULBP1 gene. The location of each binding site is given relative to the ULBP1 transcriptional start site. (C) An EMSA showing EBNA1 binding to a positive-control oligonucleotide (EBV Rep^{*} site 1; lanes 1 to 3), oligonucleotides that include ULBP1 site 1 (lanes 4 to 6) or ULBP1 site 2 (lanes 7 to 9), and a negative-control oligonucleotide (a portion of the EBV Raji origin; lanes 10 to 12). For each oligonucleotide, EBNA1 amounts added were none in the left lanes, 1.5 μ g EBNA1 in the middle lanes, and 6 μ g in the right lanes ($n = 3$; a representative image is shown). (D) Chromatin immunoprecipitation (ChIP)-qPCR measurement of EBNA1 binding to the sites identified in panel A relative to EBNA1 binding to a negative-control region in the genome (proximal to the rhodopsin gene, where there are no expected EBNA1-binding sites) in 721 lymphoblastoid cells. Data shown are relative to IgG binding at each of the sites ($n = 5$; error bars show standard error). *, $P < 0.05$.

infection is caused at least in part by the EBV latent protein EBNA1 and that this inhibition reduces NK cell-mediated killing of EBV-infected cells. EBNA1 binds many sites in the cellular genome (27, 28, 43) and can both enhance and inhibit transcription of cellular genes (44). We used a position-weighted matrix (PWM; see Fig. S1 in the supplemental material) to search for potential EBNA1-binding sites within the promoter region of the ULBP1 gene and used a position P value (described in the work of Dresang et al. [27]) cutoff of $7.7e-5$. This is the position P value associated with the lowest-affinity EBNA1-binding site in the EBV genome, Rep* site II, to which EBNA1 functionally binds (45). We found two putative EBNA1-binding sites within 5.5 kb of the ULBP1 transcription start site (TSS), one site upstream and one site downstream of the TSS (Fig. 1B). We confirmed that EBNA1 could bind these sequences using electrophoretic mobility shift assays (EMSA) (Fig. 1C) and also showed that EBNA1 binds these sites *in vivo* in the EBV-positive lymphoblastoid cell line (LCL) 721 using chromatin immunoprecipitation-quantitative PCR (ChIP-qPCR) (Fig. 1D).

To test whether loss of EBNA1 leads to increased ULBP1 expression in cells infected with EBNA1, we infected primary B cells with either wild-type EBV expressing green fluorescent protein (GFP) (wt-EBV) or a recombinant EBV null for EBNA1-expressing GFP (Δ EBNA1-EBV). Inhibiting EBNA1 in latently infected cells leads over days to the loss of EBV genomes from these cells (46, 47), causing the concomitant loss of expression of other viral genes as well. Therefore, we tested and found that in the first few days after infection with wild-type EBV and Δ EBNA1-EBV, infection dynamics were similar. Primary B cells infected with identical titers (~ 1) of these two viruses had similar fractions expressing GFP and were induced to proliferate to similar levels, as measured by B-cell blast formation (Fig. 2A). We also confirmed that equal proportions of cells were infected with virus capable of expressing viral RNAs by performing RNA *in situ* hybridization for the EBV noncoding RNAs, EBERs (Fig. 2A). Importantly, the expression of other EBV latent genes, including EBNA2, EBNA3C, and LMP1, was mostly similar in cells infected with wt-EBV or Δ EBNA1-EBV, although by day 6 postinfection EBNA3C expression had declined (Fig. S2A). However, all the effects of EBNA1 we enumerate—limiting ULBP1 and c-Myc levels as well as reduction of cellular stress responses and apoptosis—are observed by day 4 postinfection when levels of EBNA3C in B cells infected with Δ EBNA1-EBV are statistically the same as the levels seen in B cells infected with wt-EBV.

When primary B cells were infected with wt-EBV or with Δ EBNA1-EBV, ULBP1 mRNA was induced. However, ULBP1 levels were twice as high 4 days after infection with Δ EBNA1-EBV as in cells infected with wt-EBV (Fig. 2B). By 6 days postinfection, this difference increased to nearly three times more ULBP1 mRNA in primary B cells lacking EBNA1, demonstrating that EBNA1 is required to inhibit the expression of ULBP1 in newly infected B cells. To independently test whether EBNA1 alone is sufficient to decrease ULBP1 mRNA levels, we examined H1299 cells—which express ULBP1 normally—and H1299 cells expressing EBNA1. In the H1299 cells expressing EBNA1, ULBP1 mRNA levels were reduced to less than 60% of the ULBP1 levels in H1299 cells not expressing EBNA1 (Fig. 2C), indicating that EBNA1 is sufficient to inhibit ULBP1 expression. To determine the functional consequences of EBNA1's inhibition of ULBP1, we tested the susceptibility of B cells infected with wt-EBV or Δ EBNA1-EBV to NK cell-mediated killing. We measured the cytotoxicity of NK cells toward newly infected B cells by the expression of the lysosome-associated membrane protein, CD107a, on the surface of NK cells to determine their degranulation (48). Freshly isolated primary B cells were infected with wt-EBV or with Δ EBNA1-EBV, and 4 days postinfection, when ULBP1 mRNA levels are first significantly higher in cells lacking EBNA1, these newly infected cells were cocultured with autologous primary NK cells (Fig. S2B). EBV sensitizes newly infected B cells to NK cell-mediated cytotoxicity, but in the absence of EBNA1, approximately 40% more NK cells underwent degranulation when cultured with infected B cells than when they were cultured with wt-EBV-infected B cells (Fig. 2D). Importantly, the increased NK cell sensitivity to Δ EBNA1-EBV-infected cells was abrogated in the presence of blocking NKG2D antibody (Fig. 2D), showing the specificity of the assay and confirming that increased levels of ULBP1 RNA

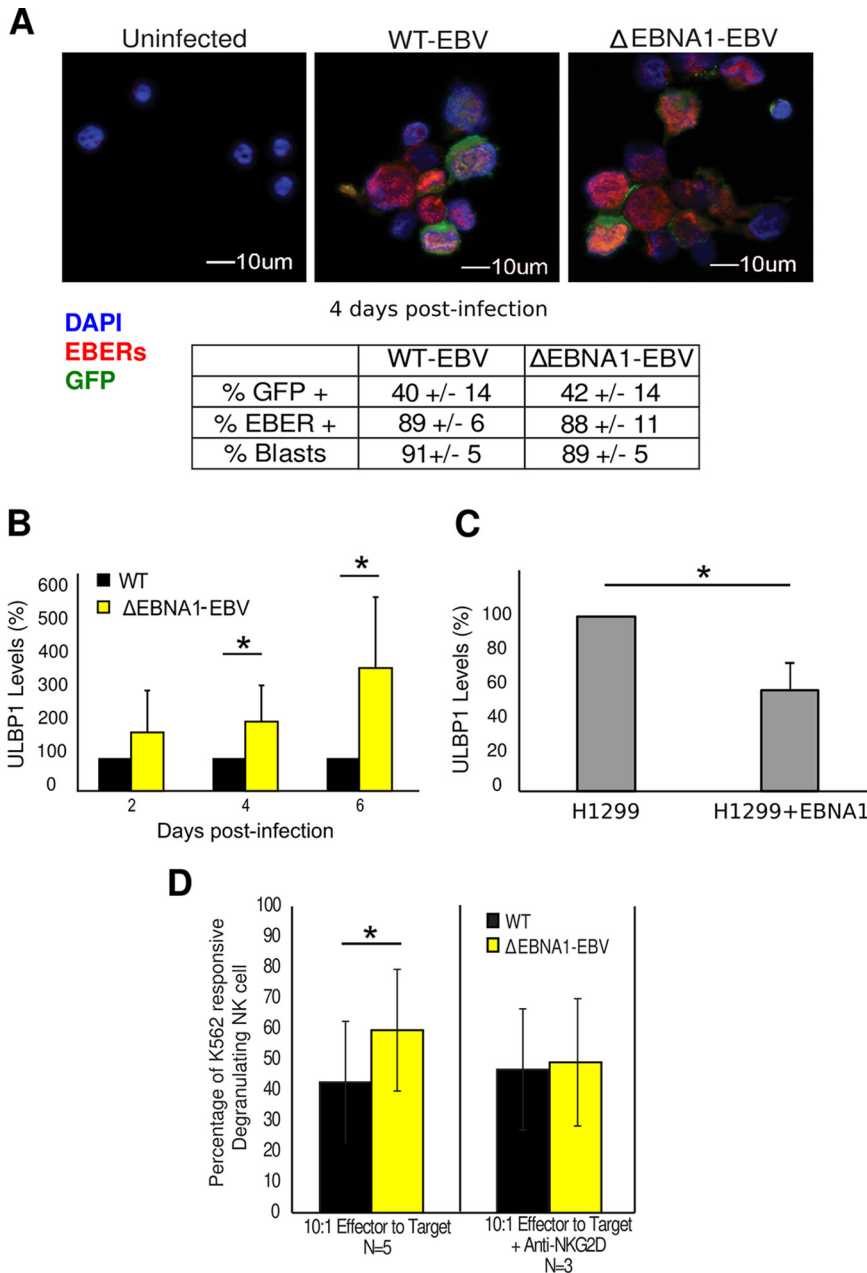


FIG 2 EBNA1 inhibits ULBP1 expression, which protects newly infected cells from NK cell-mediated killing. (A) Primary B cells infected with either wt-EBV or Δ EBNA1-EBV at equal infection rates as determined by EBERS *in situ* hybridization (red), GFP expression (green), and blast formation. The mean percentages of cells positive for each marker 4 days postinfection are provided \pm standard deviations. At least 50 cells were counted for each condition. (B) Levels of ULBP1 mRNA quantified by qRT-PCR and normalized to TBP expression at different time points following B-cell infection with wt-EBV or Δ EBNA1-EBV. The levels of ULBP1 mRNA were set to 100% for wt-EBV-infected cells ($n = 3$; error bars show standard error). (C) Expression of ULBP1 mRNA in H1299 cells and H1299 cells expressing EBNA1 quantified by qRT-PCR and normalized to GAPDH expression. The levels of ULBP1 mRNA were set to 100% in cells not expressing EBNA1 ($n = 2$; error bars show standard error). (D) NK cell cytotoxicity with B cells 4 days after infection with wt-EBV or Δ EBNA1-EBV (target cells) cocultured at a 1:10 ratio with interleukin-2 (IL-2)-stimulated NK cells (effector cells) in the presence or absence of blocking anti-NKG2D antibody. Data are presented after normalization against uninfected cells and given as the percentage of degranulating cells where response to K562 cells is 100% degranulation ($n = 5$; error bars show standard error). *, $P < 0.05$.

detected in these cells correspond to increased levels of the encoded ligand protein. These findings demonstrate that EBNA1 both inhibits ULBP1 expression in EBV-infected B cells and reduces these cells' susceptibility to NK cell-mediated cytotoxicity; together these functions promote EBV's evasion of host innate immunity *in vivo*.

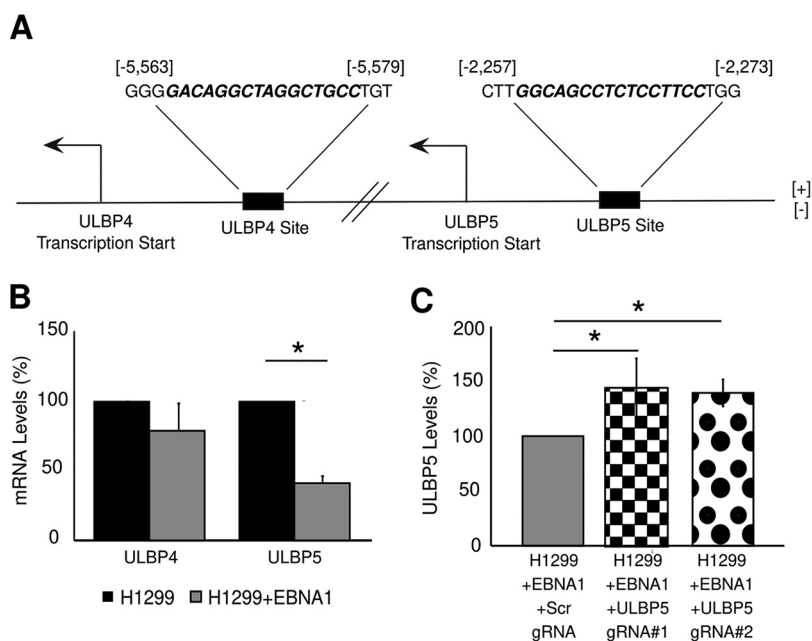


FIG 3 EBNA1 also inhibits the expression of ULBP5, another NKG2D ligand. (A) EBNA1 PWM-predicted binding sites (bold italic sequences) associated with the NKG2D ligand ULBP4 and ULBP5 genes. The location of each binding site is given relative to the ULBP4 and ULBP5 transcriptional start sites. (B) Levels of ULBP4 and ULBP5 mRNA quantified by qRT-PCR and normalized to GAPDH in H1299 cells and H1299 cells expressing EBNA1. The levels of ULBP4 and ULBP5 mRNAs were set to 100% in H1299 cells not expressing EBNA1 ($n = 3$; error bars show standard error). (C) Expression of ULBP5 mRNA in H1299 cells expressing EBNA1 with and without CRISPR-Cas9-induced mutations in the EBNA1-binding site close to the ULBP5 transcriptional start site quantified by qRT-PCR and normalized to GAPDH expression. The level of ULBP5 mRNA was set to 100% in H1299 cells expressing EBNA1 without any CRISPR-Cas9-induced mutations ($n = 3$; error bars show standard error). *, $P < 0.05$.

EBNA1 also inhibits the expression of ULBP5, another NKG2D ligand. EBV infects both B cells and epithelial cells *in vivo*, and some NKG2D ligands are expressed primarily on cells of epithelial origin. For example, ULBP4 is expressed mainly in cells derived from the ectoderm, including skin cells and cells lining the mouth and esophagus (49, 50), and ULBP5 mRNA was detected only in cells of epithelial or endocrine origin (51). We used the PWM noted earlier to scan for EBNA1-binding sites near the TSS of other ULBPs and found such sites for ULBP4 and ULBP5 (Fig. 3A). Expression of ULBP4 and ULBP5 genes, which are endogenously expressed in normal oral keratinocytes (NOKs), was found to decrease 3-fold in the presence of the Akata strain of EBV (NOKs-Akata) (Fig. S3A). However, NOKs-Akata cells maintain a latency type I/II pattern of EBV gene expression in which both EBNA1 and LMP2A are expressed (52). To test specifically whether EBNA1 alone can reduce the expression of ULBP4 and ULBP5, we generated H1299 cells expressing full-length EBNA1. In H1299 cells expressing EBNA1, ULBP5—but not ULBP4—levels were reduced significantly (Fig. 3B), making it likely that EBNA1 can inhibit ULBP5 but not ULBP4 expression. To establish that EBNA1 directly inhibits ULBP5 expression by binding the predicted site near the ULBP5 TSS, we used CRISPR-Cas9 to mutate this EBNA1-binding site (Fig. S3B). In two H1299 clones expressing EBNA1 and with confirmed mutations at the EBNA1-binding site, levels of ULBP5 mRNA increased significantly compared to an H1299 clone expressing EBNA1 and with an intact EBNA1-binding site (Fig. 3C). This finding demonstrates that abrogating EBNA1 binding near the TSS of the ULBP5 gene increases its expression, further underscoring that EBNA1 directly inhibits expression of NKG2D ligands through its DNA binding activity.

EBNA1 attenuates γ H2AX levels and apoptosis after EBV infection of B cells. Expression of NKG2D ligands can also increase due to cellular stress responses, such as

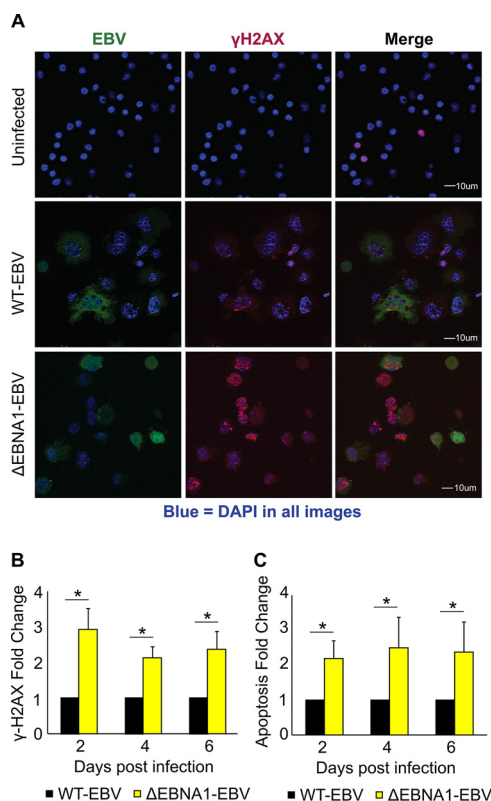


FIG 4 EBNA1 attenuates cellular stress and apoptosis after EBV infection of B cells. (A) Representative immunofluorescence images of γ H2AX foci (red) in uninfected primary B cells or B cells 4 days after infection with wt-EBV or Δ EBNA1-EBV. Green indicates GFP expression from either the recombinant wt-EBV or Δ EBNA1-EBV. (B) Fold enrichment of γ H2AX focus-positive B cells infected with Δ EBNA1-EBV relative to cells infected with wt-EBV at 2, 4, and 6 days postinfection ($n = 5$; error bars show standard error). (C) Fold enrichment of Apoligix-identified caspase-positive B cells infected with Δ EBNA1-EBV relative to cells infected with wt-EBV at 2, 4, and 6 days postinfection ($n = 5$; error bars show standard error). At least 50 cells were counted for each condition. *, $P < 0.05$.

activation of the ATR/Chk1 and ATM/Chk2 pathways, which play vital roles connected to DNA damage and replication stress (7, 8). B cells infected with EBV have been reported to activate these stress-related pathways early after infection (16–19), although more recent evidence indicates that EBV infection of B cells primarily activates the ATR/Chk1 pathway (16–18). Phosphorylation of the histone variant H2AX—forming γ H2AX—is an acknowledged marker of DNA damage and cellular stress (53). To test whether EBNA1 plays a role in limiting phosphorylation of H2AX, we infected freshly isolated, primary B cells with wt-EBV and Δ EBNA1-EBV and stained for γ H2AX and for apoptotic cells using an Apoligix apoptosis assay (Fig. 4A). The fraction of newly infected cells positive for γ H2AX more than doubled by 2 days postinfection in the absence of EBNA1, and this increase continued to be present several days postinfection (Fig. 4A and B). Likewise, the fraction of newly infected cells that exhibited active caspases more than doubled 2 days after infection with Δ EBNA1-EBV when compared to cells infected with wt-EBV (Fig. 4C). These findings show that EBNA1 reduces cellular stress responses and apoptosis, thereby promoting the survival of B cells newly infected with EBV. Furthermore, because cellular stress can increase expression of NKG2D ligands, by attenuating these phenomena, EBNA1 also likely limits expression of these ligands.

EBNA1 attenuates c-Myc levels in newly infected B cells. EBV is unique in its ability to infect and efficiently drive resting B cells to proliferate. It does so in part by increasing the expression of the c-Myc proto-oncogene. This increase in c-Myc levels is perilous, though, because it can also lead to the triggering of apoptotic signals (54)

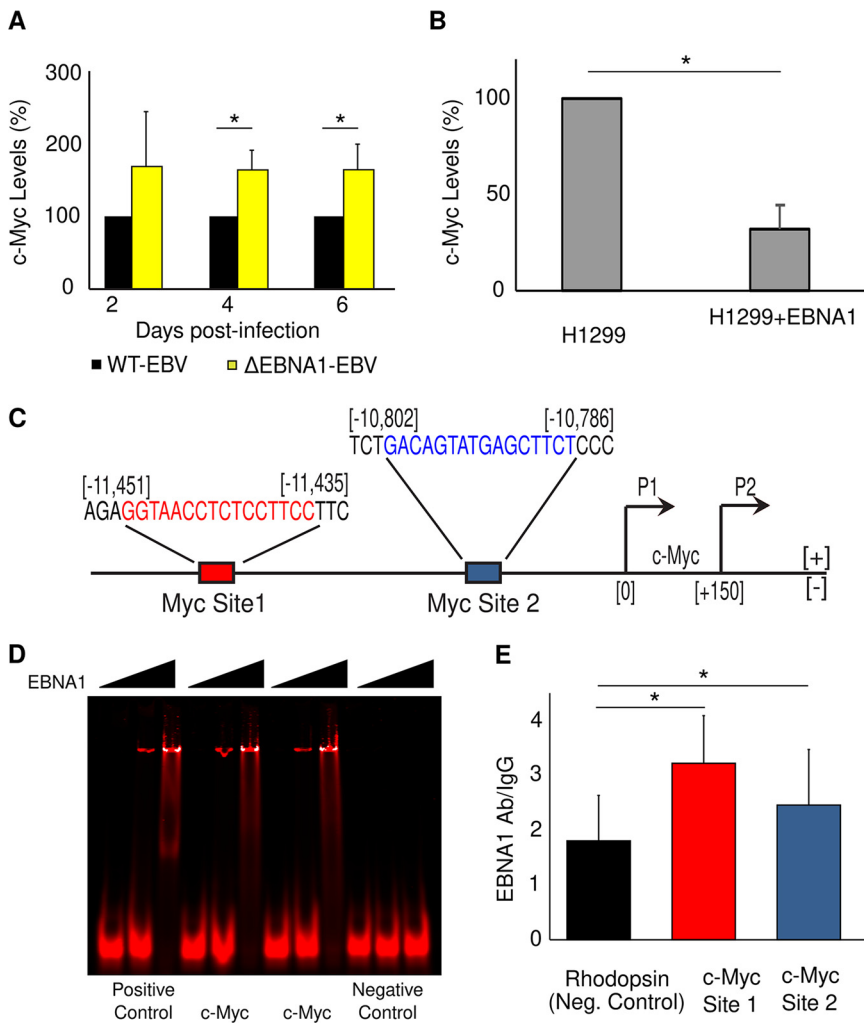


FIG 5 EBNA1 inhibits expression of c-Myc. (A) Levels of c-Myc mRNA quantified by qRT-PCR and normalized to TBP expression at different time points following B-cell infection with wt-EBV or ΔEBNA1-EBV. The levels of c-Myc mRNA were set to 100% for wt-EBV-infected cells ($n = 5$; error bars show standard error). (B) Expression of c-Myc mRNA in H1299 cells and H1299 cells expressing EBNA1 quantified by qRT-PCR and normalized to GAPDH expression. The level of c-Myc mRNA was set to 100% for cells not expressing EBNA1 ($n = 2$; error bars show standard error). (C) EBNA1 PWM-predicted binding sites (red and blue sequences) associated with the c-Myc gene. The location of each binding site is given relative to the c-Myc transcriptional start site. (D) An EMSA showing EBNA1 binding to a positive-control oligonucleotide (EBV Rep* site; lanes 1 to 3), oligonucleotides that include c-Myc site 1 (lanes 4 to 6) or c-Myc site 2 (lanes 7 to 9), and a negative-control oligonucleotide (a portion of the EBV Raji origin; lanes 10 to 12). For each oligonucleotide, EBNA1 amounts added were none in the left lanes, 1.5 μg EBNA1 in the middle lanes, and 6 μg in the right lanes ($n = 3$; a representative image is shown). (E) Chromatin immunoprecipitation (ChIP)-qPCR measurement of EBNA1 binding to the sites identified in panel C relative to EBNA1 binding to a negative-control region in the genome (proximal to the rhodopsin gene, where there are no predicted EBNA1-binding sites). Data shown are relative to IgG binding at each of the sites ($n = 5$; error bars show standard error). *, $P < 0.05$.

and in some cases increased expression of immune ligands (55). Modulating c-Myc levels could be key to balancing proliferation versus reducing apoptosis and expression of immune cell ligands, such as ULBP1. We have now found that EBV uses EBNA1 to limit c-Myc's expression in newly infected peripheral B cells. We infected B cells with wt-EBV and ΔEBNA1-EBV and found that by 4 days postinfection, c-Myc mRNA levels are 60% higher in cells infected with ΔEBNA1-EBV (Fig. 5A). We confirmed EBNA1's repression of c-Myc in H1299 cells expressing EBNA1 (Fig. 5B). Thus, while EBV induces the expression of c-Myc in newly infected primary B cells to drive proliferation, EBNA1 caps this induction of c-Myc expression. To test whether EBNA1 regulates c-Myc

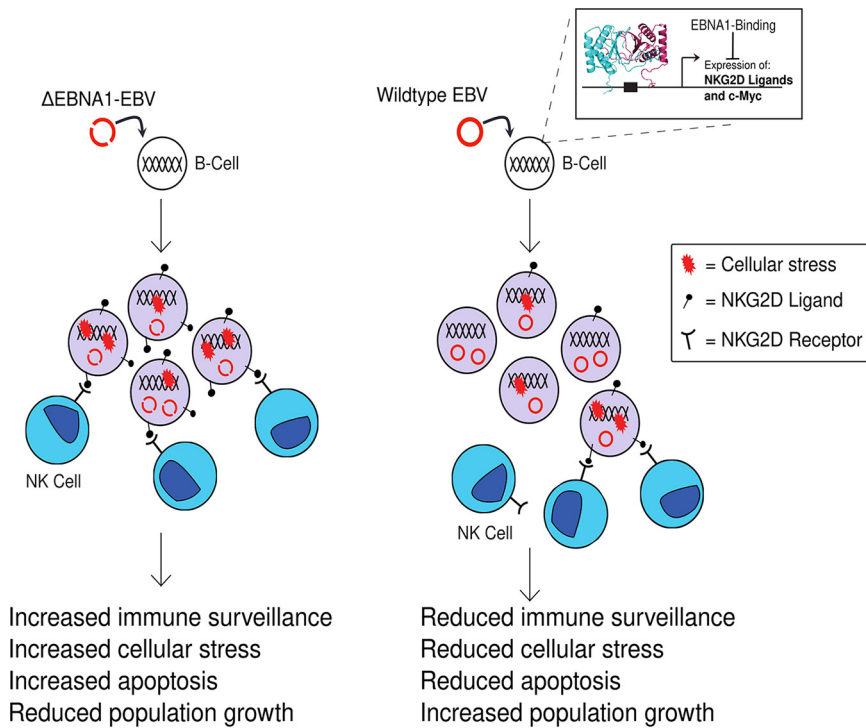


FIG 6 EBNA1 suppresses host immune response and enhances survival after infection. A model outlining how EBNA1 binds to genomic sites close to the transcriptional start site of NKG2D ligands ULBP1 and ULBP5 as well as the *c-Myc* gene and inhibits their expression. Inhibition of NKG2D ligands makes EBV-infected cells less susceptible to NK cell-mediated killing. Inhibition of *c-Myc* expression limits cellular stress responses and reduces apoptosis of newly infected cells. Limiting cellular stress can also reduce expression of immune cell ligands, further enhancing EBNA1-mediated immune evasion and survival of cells newly infected with EBV.

expression directly, we used the PWM noted above (Fig. S1) to search for potential EBNA1-binding sites within the promoter region of the *c-Myc* gene. We identified two putative EBNA1-binding sites upstream of *c-Myc*'s transcriptional start site (Fig. 5C). One of these sites (*c-Myc* site 2) was calculated to have a position *P* value of $6.7e-6$, placing its affinity among those of the cellular binding sites we have established to be bound by EBNA1 at physiological levels (27). EMSAs as well as ChIP followed by qPCR in the EBV-positive LCL 721 showed that EBNA1 binds the *c-Myc* promoter at both the predicted sites at significantly higher levels than at a genomic negative-control site (Fig. 5D and E). Taken together, these findings show that EBNA1 binds the *c-Myc* promoter region in latently infected cells and limits expression of this oncogene in newly infected B cells.

In summary, we show that in B cells newly infected with EBV, EBNA1 downregulates the NKG2D ligand ULBP1 by directly binding near its TSS. EBNA1 can also directly downregulate other NKG2D ligands, such as ULBP5. Downregulating NKG2D ligands makes EBV-infected cells less susceptible to NK cell-mediated killing. In addition to directly reducing levels of NKG2D ligands, EBNA1 downregulates cellular responses to stress and/or DNA damage—as measured by γ H2AX—after EBV infection of B cells and reduces apoptosis in newly infected cells. EBNA1 does so, at least in part, by binding to the promoter region of the *c-Myc* gene and capping its expression in newly infected peripheral B cells. Thus, we show that EBNA1 can suppress the host innate immune response through multiple pathways to increase the survival of newly infected cells (Fig. 6).

DISCUSSION

Infection with EBV elicits strong adaptive and innate immune responses (56, 57). For example, primary infection with EBV can lead to a massive expansion of viral

antigen-specific CD8⁺ T cells (14) and the accumulation of specific subtypes of natural killer (NK) cells in the tonsillar area (15), typically the site of initial EBV infection. However, some B cells newly infected with EBV manage to slip past host immune surveillance and establish a lifelong latent infection in more than 95% of the world's adult population (12). We have examined this immune evasion with a derivative of EBV that lacks the key latent protein EBNA1. EBV, in part through EBNA1, subtly regulates components of the innate immune system and cellular stress response, ensuring that some newly infected B cells evade the immune system and survive to persist for the life of the host.

Insightful studies have established that the NKG2D receptor expressed on NK cells and CD8⁺ T cells helps to control EBV infections (58, 59). Individuals who have null mutations in the magnesium transporter 1 (*MAGT1*) gene have NK cells that express severely reduced levels of NKG2D and are both susceptible to uncontrolled chronic EBV infection and more likely to develop EBV-related malignancies (58). We show that EBNA1 directly downregulates the NKG2D ligands ULBP1 and ULBP5. Importantly, the downregulation of ULBP1—and potentially also ULBP5—has vital functional consequences for EBV-infected cells as higher levels of the NKG2D ligand lead to significantly increased recognition and killing of EBV-positive cells by NK cells. It has also been found that overexpression of the EBV microRNA (miRNA) MiR-BART2-5p reduced expression of the NKG2D ligand MICB in RKO colon carcinoma cells, and a sponge directed against this miRNA led to an increase in MICB levels in the EBV-positive LCL 721, rendering these cells more susceptible to NK cell-mediated killing (23). Another study (24) showed that B cells infected with EBV lacking the latent protein LMP2A expressed significantly higher levels of the NKG2D ligand ULBP4 than did B cells infected with wt-EBV. The B cells expressing higher levels of ULBP4 were killed more efficiently by CD8⁺ T cells, but the activity of NK cells was not explored. That LMP2A can regulate expression of ULBP4 could explain why in our study NOKs cells infected with Akata-EBV showed downregulation of both ULBP4 and ULBP5, but H1299 cells expressing EBNA1 downregulated only ULBP5; NOKs-Akata cells express both EBNA1 and LMP2A (52). Unsurprisingly, EBV seems to have evolved multiple pathways to regulate the host immune response, especially in the first days after infection (20, 25). For example, Nikitin et al. (19) observed an increase of about 1.5-fold in the number of cells positive for γ H2AX foci when B cells were infected with EBNA3C-null EBV compared to infections with wt-EBV. The B cells we infect with EBNA1-null EBV still express EBNA3C (to 60% of wt levels at day 4 postinfection), yet we see close to a 3-fold increase in cells positive for γ H2AX foci when B cells are infected with EBNA1-null EBV compared to infections with wt-EBV. We reason that this finding strongly supports a role for EBNA1 (likely in cooperation with EBNA3C) in attenuating activation of γ H2AX postinfection. However, unlike LMP2A and EBNA3C, EBNA1 is expressed by all EBV-positive cells (60). EBNA1's presence in all EBV-positive cells, both early and late after infection, further highlights the importance of EBNA1's ability to directly downregulate NKG2D ligands and assist EBV-positive cells in continuing to evade immune surveillance.

In addition to avoiding detection by the immune system, B cells newly infected with EBV must balance proliferation against cellular stress and apoptosis. Infection with EBV induces naive B cells to enter the cell cycle and transition from G₀ to G₁ (61) by upregulating the expression of cellular genes, such as the oncoprotein c-Myc (62), as well as EBV's transforming genes, including EBNA1 (13). However, the robust cellular proliferation that EBV induces, in part via c-Myc expression, also activates cellular stress responses (16, 17, 19), which can upregulate expression of NKG2D ligands (7), again raising the specter of immune detection and death of these infected cells. We show that B cells infected with Δ EBNA1-EBV have higher levels of c-Myc and apoptosis and show higher numbers of γ H2AX-positive cells than B cells infected with wt-EBV, indicating that EBNA1 plays an important role in both limiting c-Myc expression and dampening cellular stress responses and apoptosis, increasing the likelihood that some EBV-infected cells survive and evade the immune system. Levels of c-Myc mRNA

in H1299 cells expressing EBNA1 were less than 33% of c-Myc levels in H1299 cells not expressing EBNA1. This difference in c-Myc levels with and without EBNA1 is significant at the steady-state level as cells often need to regulate levels of c-Myc precisely to avoid death and continue to proliferate (63).

Cellular γ H2AX is most widely known as a marker for DNA damage, but γ H2AX foci can develop even in the absence of a DNA damage response. For example, serum starvation—which is not known to cause DNA strand breaks—leads to the formation of γ H2AX foci in HaCaT cells and mouse embryonic fibroblasts in a p38-dependent manner (64). Others have shown cell cycle-dependent phosphorylation of γ H2AX in a CHK2/DNA-PKcs-dependent manner even in the absence of DNA damage (65). In the context of EBV infection of B cells, several reports have observed increased levels of γ H2AX in B cells postinfection, but whether the ATR/Chk1 or the ATM/Chk2 pathway leads to the activation of H2AX is controversial. Nikitin et al. (19) observed activation of ATM/Chk2 after EBV infection of peripheral B cells with EBV, but Mordasini et al. (16) observed only ATR/Chk1 activation after infection of peripheral or tonsillar B cells with EBV. Koganti et al. (18) showed ATR activation and STAT3-mediated interruption of the ATR/Chk1 signaling axis after EBV infection of primary B cells. More recently, Pich et al. (17) tested small-molecule inhibitors of ATM and ATR, kinases that ultimately activate γ H2AX in response to different stresses. They showed that a small-molecule inhibitor of ATM, which is activated primarily in response to DNA damage, did not reduce the fluorescent intensity of γ H2AX foci in EBV-infected B cells. In contrast, a small-molecule inhibitor of ATR, which is activated in response to persistent single-stranded DNA, especially at stalled replication forks during DNA replication stress, reduced γ H2AX levels in EBV-infected B cells. We confirmed that the downstream measure of either the ATR/Chk1 or the ATM/Chk2 pathway being activated, i.e., increased levels of γ H2AX, was significantly lower in B cells infected with wt-EBV compared to γ H2AX levels in B cells infected with Δ EBNA1-EBV, strongly indicating that the presence of EBNA1 reduces cellular stress responses in EBV-infected B cells. Future experiments can tease out which pathways are activated when B cells are infected with Δ EBNA1-EBV.

Some previous research on the relationship between EBNA1, c-Myc, and stress responses in B cells newly infected with EBV seemed to indicate that EBNA1 is dispensable for the initial survival and proliferation of the infected cells (17). The differences between these prior findings and our results likely reflect our use of peripheral B cells and the use of adenoidal B cells by Pich et al. (17). There can be significant differences in the growth and survival dynamics of adenoidal versus peripheral B cells infected with EBV, with adenoidal B cells typically showing faster growth and less death after EBV infection (66). Additionally, Pich et al. (17) examined different characteristics—activation, cell cycle entry, and proliferation—of newly infected B cells compared to our assays testing apoptosis and cellular stress response in the newly infected cells.

Extensive evidence exists showing EBNA1 can bind cellular DNA and regulate cellular gene expression both positively and negatively (reviewed in the work of Wilson et al. [67]). However, the mechanisms by which EBNA1 modulates cellular transcription are not completely clear. EBNA1 can mediate DNA looping of both viral and cellular DNAs (68, 69), and EBV-negative cells transfected with EBNA1 or engineered to express derivatives of EBNA1 develop more regions of open chromatin (70), either of which could be mechanisms by which EBNA1 affects transcription. Genome-wide assays for EBNA1 binding and transcription modulation have shown EBNA1 binding to chromatin with both active and repressive marks (36, 71), which could indicate that EBNA1 also serves as a cofactor for cellular proteins that activate or repress transcription. Indeed, EBNA1 is known to interact with several such proteins, including P32/TAP (72), nucleolin (73), nucleosome assembly factor 1 (NAP1), and template activator factor I (TAF-I) (74) among others. While we do not yet know exactly how EBNA1 downregulates the expression of NKG2D ligands or c-Myc in newly infected B cells, establishing its direct role at these genomic locations allows future experiments to elucidate how EBNA1 suppresses transcription.

Importantly, our experiments were carried out primarily in B cells newly infected with wt-EBV or Δ EBNA1-EBV and not in LCLs. LCLs have served as a powerful *in vitro* model of EBV infection and persistence but are selected for their growth in the absence of any immune selection. By focusing on the first few days postinfection, we have avoided this potential bias and been able to unearth how the EBV oncoprotein EBNA1—in addition to being indispensable for the maintenance of the viral genome in latently infected cells—contributes unexpectedly to cells newly infected with EBV by limiting their immune detection and balancing proliferation and stress responses to ultimately establish lifelong infection in hosts.

MATERIALS AND METHODS

Cell lines. Daudi (75), 721 (76), H1299 (77), HEK293 (78), K562 (79), and NOKs and NOKs-Akata (80) cells have been described previously. Additional details are given in Text S1 in the supplemental material.

Analysis of RNA-seq data. We used publicly available data derived from <http://ebv-b.helmholtz-muenchen.de> (42) to analyze the expression of NKG2D ligands before and 2, 4, and 8 days after EBV infection of B cells *in vitro*. Genes with an average expression lower than 25 normalized counts were excluded from further analyses.

Predicting EBNA1 binding. The 16-nucleotide PWM for the binding site of EBNA1 was created using the online software MEME (<http://meme.nbcr.net/meme/>) with the sequences of 73 identified EBNA1-binding sites (27). Additional details are given in Text S1.

EMSA. EMSAs were carried out using IR700-labeled oligonucleotides ordered from Integrated DNA Technologies (IDT) and recombinant EBNA1 protein from Abcam (ab138345). Labeled oligonucleotides were dimerized by dilution to 20 pmol/ μ l in 1 \times Tris-EDTA (TE), heating to 100°C for 5 min, and cooling slowly to room temperature. Indicated amounts of the EBNA1 protein and 1 μ l of a 1:100 dilution of dimerized oligonucleotides was used for the EMSAs. Five percent polyacrylamide gels were used for electrophoresis, and gels were visualized using a Li-Cor Odyssey imager. More details, including sequences of the oligonucleotides used (Table S3), are provided in the supplemental material.

Chromatin immunoprecipitation. Cells were cross-linked in 1% methanol-free formaldehyde, quenched with 0.5 M glycine, washed twice with ice-cold phosphate-buffered saline (PBS), and then lysed in the presence of a protease inhibitor cocktail (Roche). Chromatin was sheared to fragments 300 to 500 bp in size, and sonicated chromatin from 5×10^6 cell equivalents was precleared and incubated with either anti-EBNA1 (81) or isotype-matched IgG overnight, after which protein A/G beads (Pierce) conjugated with rabbit anti-rat antibody were added. Samples were then placed on a magnetic rack and washed serially. Antibody-bound chromatin was then eluted from the magnetic beads, and cross-links were reversed. Chromatin was treated with RNase and extracted by phenol, chloroform, and Qiagen PCR cleanup Kits. Isolated chromatin was analyzed by qPCR with primer and probe sets listed in Table S1. Additional details are given in Text S1.

Primary B-cell isolation. Peripheral blood mononuclear cells (PBMCs) were isolated from whole blood or buffy coat (Interstate Blood Bank Inc.) by centrifugation over a cushion of Ficoll-Paque. Platelets were removed from PBMCs by repeated washes with phosphate-buffered saline (PBS)–EDTA–fetal bovine serum (FBS). B cells were negatively isolated from PBMCs using the magnetically activated cell sorting (MACS) B-cell isolation kit II (Miltenyi Biotec). Natural killer cells were positively selected using MACS CD56 microbeads (Miltenyi Biotec).

EBER *in situ* hybridization. Cells were washed in 1 \times PBS, spread onto slides, fixed with 4% paraformaldehyde, and then permeabilized with 0.5% Triton X-100. *In situ* hybridization was carried out as described previously (82) with the use of biotinylated 30-mer oligonucleotides for EBER detection (PanPath PLB101). Hybridized probe was detected with a solution containing streptavidin conjugated to Cy3 (Cytocell). Cellular DNA was counterstained with mounting medium containing 4',6-diamidino-2-phenylindole (DAPI) (Vector). Cells were imaged using a Zeiss ApoTome.

RNA isolation, reverse transcription, and real-time qPCR (RT-qPCR). Total RNA was isolated using either the RNeasy MiniPrep Kit (Qiagen) or the Direct-zol RNA purification kit (Zymo) and included a DNase treatment according to manufacturer's instructions.

After isolation, 1 to 2 μ g of total RNA was reverse transcribed using the Applied Biosystems high-capacity reverse transcription kit with MultiScribe murine leukemia virus (MuLV) reverse transcriptase. Instead of the supplied random primer, 5 μ M 20-mer oligo(dT) was used. RT-qPCR was carried out as previously described (83). Primary B-cell and H1299 mRNA levels were normalized to TATA box-binding protein (TBP) and glyceraldehyde-3-phosphate dehydrogenase (GAPDH), respectively, and fold enrichment was determined using the threshold cycle ($\Delta\Delta C_T$) method (84). Primers and probes used are listed in Table S2.

Natural killer cell degranulation assay. Primary NK cells were treated with IL-2 (10 ng/ml BioLegend) overnight and plated at an effector-to-target ratio of 10:1 with autologous untreated B cells or autologous B cells that had been infected 4 days prior with wt-EBV or Δ EBNA1-EBV. As a positive control, NK cells were also cultured with K562 cells, which lack MHC class I and II molecules but retain NKG2D ligand expression. For antibody blocking experiments, NK cells were treated with 50 μ g/ml NKG2D blocking antibody (R&D Systems MAB139) for 30 min at room temperature prior to cultivation with target cells. NK cell degranulation assays were performed as previously described (48) with the antibodies CD56-allophycocyanin (APC) (BioLegend), CD107a-phycoerythrin (PE) (BioLegend), and CD19-fluorescein isothiocyanate

(FITC) (BioLegend). Flow cytometric analysis of live cells was performed on a FACSAria III equipped with 403-nm, 488-nm, 561-nm, and 637-nm lasers. A total of 30,000 to 60,000 events was acquired and analyzed using FlowJo software. The analysis was performed on gated cells that were characteristic of the lymphocyte population. This population was then gated for CD19⁺ CD56⁺ NK cells. Within this population the expression of CD107a was determined.

Generating mutants using CRISPR-Cas9. The CRISPR Design tool (crispr.mit.edu) was used to identify potential target sequences at EBNA1-binding sites. Spacers were synthesized by Integrated DNA Technologies (Coralville, IA), phosphorylated and annealed, and then cloned into pSpCas9(BB)-2A-GFP (PX458) (85), a gift from Feng Zhang (Addgene plasmid no. 48138). Constructs were verified by Sanger sequencing and transfected into H1299 cells with Lipofectamine 3000 (Life Technologies). Sequences targeted by guide RNAs near the ULBP5 TSS were amplified by PCR, cloned into PCR-Blunt (Invitrogen), and verified by sequencing.

Immunofluorescence staining. B cells were spread on a microscope slide, fixed in 4% paraformaldehyde (PFA), and then permeabilized with 0.5% Tween 20 and blocked with 5% normal goat serum. Additional details and antibodies used are listed in Text S1.

Apoptosis detection. The Apoptosis assay for detection of apoptosis was carried out as previously described (86). Briefly, cells were stained with SR-VAD-FMK (SR100; Cell Technology Inc) or FAM-VAD-FMK (FAM100; Cell Technology Inc) following the manufacturer's protocol with two alterations. First, the cells were stained at an 0.5× final concentration of SR-VAD-FMK or FAM-VAD-FMK rather than at a 1× final concentration. Second, cells were washed in 1× PBS rather than the manufacturer's supplied wash buffer. After staining, cells were fixed using a 1× final concentration of fixative solution supplied by the manufacturer. Cells were analyzed and counted on an inverted fluorescence microscope (Axiovert 200M; Zeiss) using the Texas Red and FITC filter sets.

Statistics. Microsoft Excel and Mstat 5.5 were used for statistical analysis. All statistics reported are the results of a two-sided Student *t* test, unless otherwise stated.

SUPPLEMENTAL MATERIAL

Supplemental material is available online only.

TEXT S1, DOCX file, 0.02 MB.

FIG S1, DOCX file, 0.3 MB.

FIG S2A, DOCX file, 0.01 MB.

FIG S2B, DOCX file, 0.1 MB.

FIG S3A, DOCX file, 0.02 MB.

FIG S3B, DOCX file, 0.03 MB.

TABLE S1, DOCX file, 0.02 MB.

TABLE S2, DOCX file, 0.02 MB.

TABLE S3, DOCX file, 0.01 MB.

ACKNOWLEDGMENTS

This research was supported in part by funding from the National Cancer Institute, National Institutes of Health (grants P01 CA022443, R01 CA133027, R01 CA070723, and T32 CA009135) and the University of Wisconsin Carbone Cancer Center support grant P30 CA014520, specifically the UWCCC Small Molecule Screening Facility and the UWCCC Flow Cytometry Laboratory. B.S. is an American Cancer Society Research Professor.

We thank Arthur Sugden for help with the BIND prediction program and our laboratory colleagues for their help and suggestions with the manuscript.

D.W.S., A.C., M.H., and B.S. designed the research; W.H. and B.S. provided reagents; D.W.S., A.C., B.S., and M.H. performed the research and collected and analyzed the data; D.W.S., A.C., and B.S. wrote the manuscript with inputs from W.H. and M.H.

The author(s) declare no competing financial interests or conflicts of interest.

REFERENCES

- Janeway CA, Jr, Travers P, Walport M, Shlomchik MJ. 2001. Immunobiology: the immune system in health and disease, 5th ed. Garland Science, New York, NY.
- Gasteiger G, D'Oswaldo A, Schubert DA, Weber A, Bruscia EM, Hartl D. 2017. Cellular innate immunity: an old game with new players. *J Innate Immunol* 9:111–125. <https://doi.org/10.1159/000453397>.
- Zhang Y, Huang B. 2017. The development and diversity of ILCs, NK cells and their relevance in health and diseases. *Adv Exp Med Biol* 1024: 225–244. https://doi.org/10.1007/978-981-10-5987-2_11.
- Abel AM, Yang C, Thakar MS, Malarkannan S. 2018. Natural killer cells: development, maturation, and clinical utilization. *Front Immunol* 9:1869. <https://doi.org/10.3389/fimmu.2018.01869>.
- Wensveen FM, Jelenčić V, Polić B. 2018. NKG2D: a master regulator of immune cell responsiveness. *Front Immunol* 9:441. <https://doi.org/10.3389/fimmu.2018.00441>.
- Mistry AR, O'Callaghan CA. 2007. Regulation of ligands for the activating receptor NKG2D. *Immunology* 121:439–447. <https://doi.org/10.1111/j.1365-2567.2007.02652.x>.

7. Gasser S, Orsulic S, Brown EJ, Raulet DH. 2005. The DNA damage pathway regulates innate immune system ligands of the NKG2D receptor. *Nature* 436:1186–1190. <https://doi.org/10.1038/nature03884>.
8. Raulet DH, Gasser S, Gowen BG, Deng W, Jung H. 2013. Regulation of ligands for the NKG2D activating receptor. *Annu Rev Immunol* 31:413–441. <https://doi.org/10.1146/annurev-immunol-032712-095951>.
9. Odom CI, Gaston DC, Markert JM, Cassidy KA. 2012. Human herpesviridae methods of natural killer cell evasion. *Adv Virol* 2012:359869. <https://doi.org/10.1155/2012/359869>.
10. De Pelsmaeker S, Romero N, Vitale M, Favoreel HW. 2018. Herpesvirus evasion of natural killer cells. *J Virol* 92:e02105-17. <https://doi.org/10.1128/JVI.02105-17>.
11. Della Chiesa M, De Maria A, Muccio L, Bozzano F, Sivori S, Moretta L. 2019. Human NK cells and herpesviruses: mechanisms of recognition, response and adaptation. *Front Microbiol* 10:2297. <https://doi.org/10.3389/fmicb.2019.02297>.
12. Sugden B. 2014. Epstein-Barr virus: the path from association to causality for a ubiquitous human pathogen. *PLoS Biol* 12:e1001939. <https://doi.org/10.1371/journal.pbio.1001939>.
13. Kang M-S, Kieff E. 2015. Epstein-Barr virus latent genes. *Exp Mol Med* 47:e131. <https://doi.org/10.1038/emmm.2014.84>.
14. Callan MF, Tan L, Annel N, Ogg GS, Wilson JD, O'Callaghan CA, Steven N, McMichael AJ, Rickinson AB. 1998. Direct visualization of antigen-specific CD8+ T cells during the primary immune response to Epstein-Barr virus in vivo. *J Exp Med* 187:1395–1402. <https://doi.org/10.1084/jem.187.9.1395>.
15. Lünemann A, Vanoaica LD, Azzi T, Nadal D, Münz C. 2013. A distinct subpopulation of human NK cells restricts B cell transformation by EBV. *J Immunol* 191:4989–4995. <https://doi.org/10.4049/jimmunol.1301046>.
16. Mordasini V, Ueda S, Aslandogmus R, Berger C, Gysin C, Hühn D, Sartori AA, Bernasconi M, Nadal D. 2017. Activation of ATR-Chk1 pathway facilitates EBV-mediated transformation of primary tonsillar B-cells. *Oncotarget* 8:6461–6474. <https://doi.org/10.18632/oncotarget.14120>.
17. Pich D, Mrozek-Gorska P, Bouvet M, Sugimoto A, Akidil E, Grundhoff A, Hamperl S, Ling PD, Hammerschmidt W. 2019. First days in the life of naive human B lymphocytes infected with Epstein-Barr virus. *mBio* 10:e01723-19. <https://doi.org/10.1128/mBio.01723-19>.
18. Koganti S, Hui-Yuen J, McAllister S, Gardner B, Grasser F, Palendira U, Tangye SG, Freeman AF, Bhaduri-McIntosh S. 2014. STAT3 interrupts ATR-Chk1 signaling to allow oncovirus-mediated cell proliferation. *Proc Natl Acad Sci U S A* 111:4946–4951. <https://doi.org/10.1073/pnas.1400683111>.
19. Nikitin PA, Yan CM, Forte E, Bocedi A, Tourigny JP, White RE, Allday MJ, Patel A, Dave SS, Kim W, Hu K, Guo J, Tainter D, Rusyn E, Luftig MA. 2010. An ATM/Chk2-mediated DNA damage-responsive signaling pathway suppresses Epstein-Barr virus transformation of primary human B cells. *Cell Host Microbe* 8:510–522. <https://doi.org/10.1016/j.chom.2010.11.004>.
20. Reising ME, Horst D, Griffin BD, Tellam J, Zuo J, Khanna R, Rowe M, Wiertz EJHJ. 2008. Epstein-Barr virus evasion of CD8+ and CD4+ T cell immunity via concerted actions of multiple gene products. *Semin Cancer Biol* 18:397–408. <https://doi.org/10.1016/j.semcancer.2008.10.008>.
21. Kalla M, Hammerschmidt W. 2012. Human B cells on their route to latent infection - early but transient expression of lytic genes of Epstein-Barr virus. *Eur J Cell Biol* 91:65–69. <https://doi.org/10.1016/j.ejcb.2011.01.014>.
22. Jochum S, Moosmann A, Lang S, Hammerschmidt W, Zeidler R. 2012. The EBV immunoevasins vIL-10 and BNLF2a protect newly infected B cells from immune recognition and elimination. *PLoS Pathog* 8:e1002704. <https://doi.org/10.1371/journal.ppat.1002704>.
23. Nachmani D, Stern-Ginossar N, Sarid R, Mandelboim O. 2009. Diverse herpesvirus microRNAs target the stress-induced immune ligand MICB to escape recognition by natural killer cells. *Cell Host Microbe* 5:376–385. <https://doi.org/10.1016/j.chom.2009.03.003>.
24. Rancan C, Schirrmann L, Hüls C, Zeidler R, Moosmann A. 2015. Latent membrane protein LMP2A impairs recognition of EBV-infected cells by CD8+ T cells. *PLoS Pathog* 11:e1004906. <https://doi.org/10.1371/journal.ppat.1004906>.
25. Albanese M, Tagawa T, Buschle A, Hammerschmidt W. 2017. MicroRNAs of Epstein-Barr virus control innate and adaptive antiviral immunity. *J Virol* 91:e01667-16. <https://doi.org/10.1128/JVI.01667-16>.
26. Ambinder RF, Shah WA, Rawlins DR, Hayward GS, Hayward SD. 1990. Definition of the sequence requirements for binding of the EBNA-1 protein to its palindromic target sites in Epstein-Barr virus DNA. *J Virol* 64:2369–2379. <https://doi.org/10.1128/JVI.64.5.2369-2379.1990>.
27. Dresang LR, Vereide DT, Sugden B. 2009. Identifying sites bound by Epstein-Barr virus nuclear antigen 1 (EBNA1) in the human genome: defining a position-weighted matrix to predict sites bound by EBNA1 in viral genomes. *J Virol* 83:2930–2940. <https://doi.org/10.1128/JVI.01974-08>.
28. Lu F, Wikramasinghe P, Norseen J, Tsai K, Wang P, Showe L, Davuluri RV, Lieberman PM. 2010. Genome-wide analysis of host-chromosome binding sites for Epstein-Barr virus nuclear antigen 1 (EBNA1). *Virology* 407:262–272. <https://doi.org/10.1016/j.virol.2010.07.026>.
29. Yates JL, Warren N, Sugden B. 1985. Stable replication of plasmids derived from Epstein-Barr virus in various mammalian cells. *Nature* 313:812–815. <https://doi.org/10.1038/313812a0>.
30. Lupton S, Levine AJ. 1985. Mapping genetic elements of Epstein-Barr virus that facilitate extrachromosomal persistence of Epstein-Barr virus-derived plasmids in human cells. *Mol Cell Biol* 5:2533–2542. <https://doi.org/10.1128/mcb.5.10.2533-2542.1985>.
31. Sugden B, Warren N. 1989. A promoter of Epstein-Barr virus that can function during latent infection can be transactivated by EBNA-1, a viral protein required for viral DNA replication during latent infection. *J Virol* 63:2644–2649. <https://doi.org/10.1128/JVI.63.6.2644-2649.1989>.
32. Sample J, Henson EB, Sample C. 1992. The Epstein-Barr virus nuclear protein 1 promoter active in type I latency is autoregulated. *J Virol* 66:4654–4661. <https://doi.org/10.1128/JVI.66.8.4654-4661.1992>.
33. Sung NS, Wilson J, Davenport M, Sista ND, Pagano JS. 1994. Reciprocal regulation of the Epstein-Barr virus BamHI-F promoter by EBNA-1 and an E2F transcription factor. *Mol Cell Biol* 14:7144–7152. <https://doi.org/10.1128/mcb.14.11.7144-7152.1994>.
34. Gahn TA, Sugden B. 1995. An EBNA-1-dependent enhancer acts from a distance of 10 kilobase pairs to increase expression of the Epstein-Barr virus LMP gene. *J Virol* 69:2633–2636. <https://doi.org/10.1128/JVI.69.4.2633-2636.1995>.
35. Altmann M, Pich D, Ruiss R, Wang J, Sugden B, Hammerschmidt W. 2006. Transcriptional activation by EBV nuclear antigen 1 is essential for the expression of EBV's transforming genes. *Proc Natl Acad Sci U S A* 103:14188–14193. <https://doi.org/10.1073/pnas.0605985103>.
36. Tempura I, De Leo A, Kossenkov AV, Cesaroni M, Song H, Dawany N, Showe L, Lu F, Wikramasinghe P, Lieberman PM. 2016. Identification of MEF2B, EBF1, and IL6R as direct gene targets of Epstein-Barr virus (EBV) nuclear antigen 1 critical for EBV-infected B-lymphocyte survival. *J Virol* 90:345–355. <https://doi.org/10.1128/JVI.02318-15>.
37. Levitskaya J, Coram M, Levitsky V, Imreh S, Steigerwald-Mullen PM, Klein G, Kurilla MG, Masucci MG. 1995. Inhibition of antigen processing by the internal repeat region of the Epstein-Barr virus nuclear antigen-1. *Nature* 375:685–688. <https://doi.org/10.1038/375685a0>.
38. Yin Y, Manoury B, Fähræus R. 2003. Self-inhibition of synthesis and antigen presentation by Epstein-Barr virus-encoded EBNA1. *Science* 301:1371–1374. <https://doi.org/10.1126/science.1088902>.
39. Paludan C, Schmid D, Landthaler M, Vockerodt M, Kube D, Tuschl T, Münz C. 2005. Endogenous MHC class II processing of a viral nuclear antigen after autophagy. *Science* 307:593–596. <https://doi.org/10.1126/science.1104904>.
40. Raulet DH. 2003. Roles of the NKG2D immunoreceptor and its ligands. *Nat Rev Immunol* 3:781–790. <https://doi.org/10.1038/nri1199>.
41. Hayakawa Y, Smyth MJ. 2006. NKG2D and cytotoxic effector function in tumor immune surveillance. *Semin Immunol* 18:176–185. <https://doi.org/10.1016/j.smim.2006.03.005>.
42. Mrozek-Gorska P, Buschle A, Pich D, Schwarzmayr T, Fechtner R, Scialdone A, Hammerschmidt W. 2019. Epstein-Barr virus reprograms human B lymphocytes immediately in the prelatent phase of infection. *Proc Natl Acad Sci U S A* 116:16046–16055. <https://doi.org/10.1073/pnas.1901314116>.
43. Canaan A, Haviv I, Urban AE, Schulz VP, Hartman S, Zhang Z, Palejev D, Deisseroth AB, Lacy J, Snyder M, Gerstein M, Weissman SM. 2009. EBNA1 regulates cellular gene expression by binding cellular promoters. *Proc Natl Acad Sci U S A* 106:22421–22426. <https://doi.org/10.1073/pnas.0911676106>.
44. Kennedy G, Sugden B. 2003. EBNA-1, a bifunctional transcriptional activator. *Mol Cell Biol* 23:6901–6908. <https://doi.org/10.1128/MCB.23.19.6901-6908.2003>.
45. Wang J, Lindner SE, Leight ER, Sugden B. 2006. Essential elements of a licensed, mammalian plasmid origin of DNA synthesis. *Mol Cell Biol* 26:1124–1134. <https://doi.org/10.1128/MCB.26.3.1124-1134.2006>.
46. Kirchmaier AL, Sugden B. 1997. Dominant-negative inhibitors of EBNA-1 of Epstein-Barr virus. *J Virol* 71:1766–1775. <https://doi.org/10.1128/JVI.71.3.1766-1775.1997>.
47. Mackey D, Sugden B. 1999. The linking regions of EBNA1 are essential for its support of replication and transcription. *Mol Cell Biol* 19:3349–3359. <https://doi.org/10.1128/MCB.19.5.3349>.

48. Alter G, Malenfant JM, Altfield M. 2004. CD107a as a functional marker for the identification of natural killer cell activity. *J Immunol Methods* 294: 15–22. <https://doi.org/10.1016/j.jim.2004.08.008>.
49. Chalupny NJ, Sutherland CL, Lawrence WA, Rein-Weston A, Cosman D. 2003. ULBP4 is a novel ligand for human NKG2D. *Biochem Biophys Res Commun* 305:129–135. [https://doi.org/10.1016/S0006-291X\(03\)00714-9](https://doi.org/10.1016/S0006-291X(03)00714-9).
50. Zöller T, Wittenbrink M, Hoffmeister M, Steinle A. 2018. Cutting an NKG2D ligand short: cellular processing of the peculiar human NKG2D ligand ULBP4. *Front Immunol* 9:620. <https://doi.org/10.3389/fimmu.2018.00620>.
51. Eagle RA, Flack G, Warford A, Martínez-Borra J, Jafferji I, Traherne JA, Ohashi M, Boyle LH, Barrow AD, Caillaud-Zucman S, Young NT, Trowsdale J. 2009. Cellular expression, trafficking, and function of two isoforms of human ULBP5/RAET1G. *PLoS One* 4:e4503. <https://doi.org/10.1371/journal.pone.0004503>.
52. Birdwell CE, Queen KJ, Kilgore PCSR, Rollyson P, Trutschl M, Cvek U, Scott RS. 2014. Genome-wide DNA methylation as an epigenetic consequence of Epstein-Barr virus infection of immortalized keratinocytes. *J Virol* 88: 11442–11458. <https://doi.org/10.1128/JVI.00972-14>.
53. Mah LJ, El-Osta A, Karagiannis TC. 2010. γ H2AX: a sensitive molecular marker of DNA damage and repair. *Leukemia* 24:679–686. <https://doi.org/10.1038/leu.2010.6>.
54. Pelengaris S, Rudolph B, Littlewood T. 2000. Action of Myc in vivo - proliferation and apoptosis. *Curr Opin Genet Dev* 10:100–105. [https://doi.org/10.1016/S0959-437X\(99\)00046-5](https://doi.org/10.1016/S0959-437X(99)00046-5).
55. Huelgo-Zapico L, Acebes-Huerta A, López-Soto A, Villa-Álvarez M, Gonzalez-Rodriguez AP, Gonzalez S. 2014. Molecular bases for the regulation of NKG2D ligands in cancer. *Front Immunol* 5:106. <https://doi.org/10.3389/fimmu.2014.00106>.
56. Hatton OL, Harris-Arnold A, Schaffert S, Krams SM, Martinez OM. 2014. The interplay between Epstein-Barr virus and B lymphocytes: implications for infection, immunity, and disease. *Immunol Res* 58:268–276. <https://doi.org/10.1007/s12026-014-8496-1>.
57. Rickinson AB, Long HM, Palendira U, Münz C, Hislop AD. 2014. Cellular immune controls over Epstein-Barr virus infection: new lessons from the clinic and the laboratory. *Trends Immunol* 35:159–169. <https://doi.org/10.1016/j.it.2014.01.003>.
58. Chaigne-Delalande B, Li F-Y, O'Connor GM, Lukacs MJ, Jiang P, Zheng L, Shatzer A, Biancalana M, Pittaluga S, Matthews HF, Jancel TJ, Blesing JJ, Marsh RA, Kuijpers TW, Nichols KE, Lucas CL, Nagpal S, Mehmet H, Su HC, Cohen JI, Uzel G, Lenardo MJ. 2013. Mg²⁺ regulates cytotoxic functions of NK and CD8 T cells in chronic EBV infection through NKG2D. *Science* 341:186–191. <https://doi.org/10.1126/science.1240094>.
59. Schmiedel D, Mandelboim O. 2017. Disarming cellular alarm systems-manipulation of stress-induced NKG2D ligands by human herpesviruses. *Front Immunol* 8:390–398. <https://doi.org/10.3389/fimmu.2017.00390>.
60. Smith DW, Sugden B. 2013. Potential cellular functions of Epstein-Barr nuclear antigen 1 (EBNA1) of Epstein-Barr virus. *Viruses* 5:226–240. <https://doi.org/10.3390/v5010226>.
61. Sinclair AJ, Palmero I, Peters G, Farrell PJ. 1994. EBNA-2 and EBNA-LP cooperate to cause G0 to G1 transition during immortalization of resting human B lymphocytes by Epstein-Barr virus. *EMBO J* 13:3321–3328. <https://doi.org/10.1002/j.1460-2075.1994.tb06634.x>.
62. Kaiser C, Laux G, Eick D, Jochner N, Bornkamm GW, Kempkes B. 1999. The proto-oncogene c-myc is a direct target gene of Epstein-Barr virus nuclear antigen 2. *J Virol* 73:4481–4484. <https://doi.org/10.1128/JVI.73.5.4481-4484.1999>.
63. Levens D. 2010. You don't muck with MYC. *Genes Cancer* 1:547–554. <https://doi.org/10.1177/1947601910377492>.
64. Lu C, Shi Y, Wang Z, Song Z, Zhu M, Cai Q, Chen T. 2008. Serum starvation induces H2AX phosphorylation to regulate apoptosis via p38 MAPK pathway. *FEBS Lett* 582:2703–2708. <https://doi.org/10.1016/j.febslet.2008.06.051>.
65. Tu W-Z, Li B, Huang B, Wang Y, Liu X-D, Guan H, Zhang S-M, Tang Y, Rang W-Q, Zhou P-K. 2013. γ H2AX foci formation in the absence of DNA damage: mitotic H2AX phosphorylation is mediated by the DNA-PKcs/CHK2 pathway. *FEBS Lett* 587:3437–3443. <https://doi.org/10.1016/j.febslet.2013.08.028>.
66. Zeidler R, Meissner P, Eissner G, Lazis S, Hammerschmidt W. 1996. Rapid proliferation of B cells from adenoids in response to Epstein-Barr virus infection. *Cancer Res* 56:5610–5614.
67. Wilson J, Manet E, Gruffat H, Busson P, Blondel M, Fahraeus R. 2018. EBNA1: oncogenic activity, immune evasion and biochemical functions provide targets for novel therapeutic strategies against Epstein-Barr virus-associated cancers. *Cancers* 10:109. <https://doi.org/10.3390/cancers10040109>.
68. Middleton T, Sugden B. 1992. EBNA1 can link the enhancer element to the initiator element of the Epstein-Barr virus plasmid origin of DNA replication. *J Virol* 66:489–495. <https://doi.org/10.1128/JVI.66.1.489-495.1992>.
69. Tempera I, Klichinsky M, Lieberman PM. 2011. EBV latency types adopt alternative chromatin conformations. *PLoS Pathog* 7:e1002180. <https://doi.org/10.1371/journal.ppat.1002180>.
70. Coppotelli G, Mughal N, Callegari S, Sompallae R, Caja L, Luijsterburg MS, Dantuma NP, Moustakas A, Masucci MG. 2013. The Epstein-Barr virus nuclear antigen-1 reprograms transcription by mimicry of high mobility group A proteins. *Nucleic Acids Res* 41:2950–2962. <https://doi.org/10.1093/nar/gkt032>.
71. Arvey A, Tempera I, Tsai K, Chen H-S, Tikhmyanova N, Klichinsky M, Leslie C, Lieberman PM. 2012. An atlas of the Epstein-Barr virus transcriptome and epigenome reveals host-virus regulatory interactions. *Cell Host Microbe* 12:233–245. <https://doi.org/10.1016/j.chom.2012.06.008>.
72. Wang Y, Finan JE, Middeldorp JM, Hayward SD. 1997. P32/TAP, a cellular protein that interacts with EBNA-1 of Epstein-Barr virus. *Virology* 236: 18–29. <https://doi.org/10.1006/viro.1997.8739>.
73. Chen Y-L, Liu C-D, Cheng C-P, Zhao B, Hsu H-J, Shen C-L, Chiu S-J, Kieff E, Peng C-W. 2014. Nucleolin is important for Epstein-Barr virus nuclear antigen 1-mediated episome binding, maintenance, and transcription. *Proc Natl Acad Sci U S A* 111:243–248. <https://doi.org/10.1073/pnas.1321800111>.
74. Wang S, Frappier L. 2009. Nucleosome assembly proteins bind to Epstein-Barr virus nuclear antigen 1 and affect its functions in DNA replication and transcriptional activation. *J Virol* 83:11704–11714. <https://doi.org/10.1128/JVI.00931-09>.
75. Nanbo A, Inoue K, Adachi-Takasawa K, Takada K. 2002. Epstein-Barr virus RNA confers resistance to interferon- α -induced apoptosis in Burkitt's lymphoma. *EMBO J* 21:954–965. <https://doi.org/10.1093/emboj/21.5.954>.
76. Kavathas P, Bach FH, DeMars R. 1980. Gamma ray-induced loss of expression of HLA and glyoxalase I alleles in lymphoblastoid cells. *Proc Natl Acad Sci U S A* 77:4251–4255. <https://doi.org/10.1073/pnas.77.7.4251>.
77. Giaccone G, Battey J, Gazdar AF, Oie H, Draoui M, Moody TW. 1992. Neuromedin B is present in lung cancer cell lines. *Cancer Res* 52(9 Suppl): 2732s–2736s.
78. Graham FL, Smiley J, Russell WC, Nairn R. 1977. Characteristics of a human cell line transformed by DNA from human adenovirus type 5. *J Gen Virol* 36:59–72. <https://doi.org/10.1099/0022-1317-36-1-59>.
79. Luzzio CB, Luzzio BB. 1975. Human chronic myelogenous leukemia cell line with positive Philadelphia chromosome. *Blood* 45:321–334. <https://doi.org/10.1182/blood.V45.3.321.bloodjournal453321>.
80. Wille CK, Nawandar DM, Panfil AR, Ko MM, Hagemeyer SR, Kenney SC. 2013. Viral genome methylation differentially affects the ability of BZLF1 versus BRLF1 to activate Epstein-Barr virus lytic gene expression and viral replication. *J Virol* 87:935–950. <https://doi.org/10.1128/JVI.01790-12>.
81. Grässer FA, Murray PG, Kremmer E, Klein K, Remberger K, Feiden W, Reynolds G, Niedobitek G, Young LS, Mueller-Lantsch N. 1994. Monoclonal antibodies directed against the Epstein-Barr virus-encoded nuclear antigen 1 (EBNA1): immunohistologic detection of EBNA1 in the malignant cells of Hodgkin's disease. *Blood* 84:3792–3798. <https://doi.org/10.1182/blood.V84.11.3792.bloodjournal84113792>.
82. Femino AM, Fay FS, Fogarty K, Singer RH. 1998. Visualization of single RNA transcripts in situ. *Science* 280:585–590. <https://doi.org/10.1126/science.280.5363.585>.
83. Pratt ZL, Kuzembayeva M, Sengupta S, Sugden B. 2009. The microRNAs of Epstein-Barr virus are expressed at dramatically differing levels among cell lines. *Virology* 386:387–397. <https://doi.org/10.1016/j.virol.2009.01.006>.
84. Livak KJ, Schmittgen TD. 2001. Analysis of relative gene expression data using real-time quantitative PCR and the 2⁻(Delta Delta C(T)) method. *Methods* 25:402–408. <https://doi.org/10.1006/meth.2001.1262>.
85. Ran FA, Hsu PD, Wright J, Agarwala V, Scott DA, Zhang F. 2013. Genome engineering using the CRISPR-Cas9 system. *Nat Protoc* 8:2281–2308. <https://doi.org/10.1038/nprot.2013.143>.
86. Vereide DT, Sugden B. 2011. Lymphomas differ in their dependence on Epstein-Barr virus. *Blood* 117:1977–1985. <https://doi.org/10.1182/blood-2010-05-285791>.